on Low Temperature Physics, Boulder, Colorado, 1972 (to be published), and to be published.
[11]G. Ahlers, Phys. Rev. 171, 275 (1968).
[12]G. Ahlers, J. Low Temp. Phys. 1, 609 (1969).
[13]The temperature dependence of Δu is mainly determined by the behavior of $1/C_p{}^2$. The exponent of the weaker term, $\epsilon^{0.022}$, was evaluated from the data of G. Ahlers [Phys. Rev. A 3, 696 (1971)] invoking scaling laws.
[14]Ahlers, Ref. 13.
[15]The attenuation data were analyzed neglecting the temperature dependence of Δu (Ref. 3). An analysis with the PK theory (Ref. 5) leads to a maximum at $\omega\tau < 1$. Taking the temperature dependence of Δu into account strongly influences the value of the relaxation time τ. Such an analysis does not affect the calculated PK dispersion by more than the errors quoted above for A. The conclusions in this Letter about the dispersion are not influenced by the details of the analysis of the attenuation data.

Instability of an Unneutralized Relativistic Electron Beam

Y. Carmel and J. A. Nation
Laboratory of Plasma Studies and School of Electrical Engineering, Cornell University, Ithaca, New York 14850
(Received 26 April 1973)

Experimental observations of the propagation of an intense, unneutralized, annular, relativistic electron beam along a homogeneous magnetic guide field show that it is unstable. The instability is accompanied by a loss of beam particles and intense microwave emission.

High-current relativistic electron beams are now being used in both plasma heating and confinement experiments.[1-4] While these experiments use neutralized electron beams, the diode and injection regions can be unneutralized. Techniques now exist for the production and transport of low-impedence, electrostatically unneutralized beams.[5,6] We describe a series of experiments investigating the stability of an unneutralized electron beam similar to that described by Friedman and Ury[7] and also used in microwave generation experiments.[8,9] In the experiments reported here the operation is at relatively high impedance with beam energies of 400 keV, diode currents of up to 30 kA, and pulse durations of 60 nsec. The beam is an annulus with a 3.8-cm diameter and a thickness of 0.2 cm. It is propagated along a magnetic guide field through a 3-m–long metallic drift tube of 5.0-cm diameter. The base pressure in the drift tube is below 5×10^{-5} Torr.

Figure 1 shows Lucite witness plates mounted at different positions along the drift tube for a guide-field strength of 8 kG. The beam thickness has grown from its initial value of about 1.5 mm at injection to 3.0 mm at the first witness-plate location. Within the next 0.75 m the beam expands radially inward until it fills the central part of the tube. As seen in Fig. 1, the filling is not completely uniform but exhibits an azimuthal structure with seven or eightfold azimuthal variation. This feature is always present but not extremely well defined or completely repeatable as regards the azimuthal mode number. A more quantitative estimate of the expansion rate is shown in Fig. 2 which plots the thickness of the annular beam as a function of the ax-

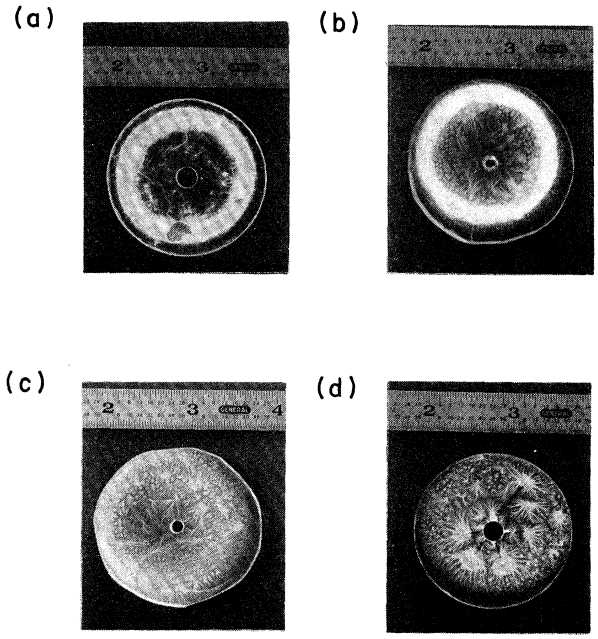

FIG. 1. Witness plates mounted at (a) 0.75 m, (b) 1.2 m, (c) 1.5 m, and (d) 3.0 m along the drift tube. The beam remained centered in the tube in all cases.

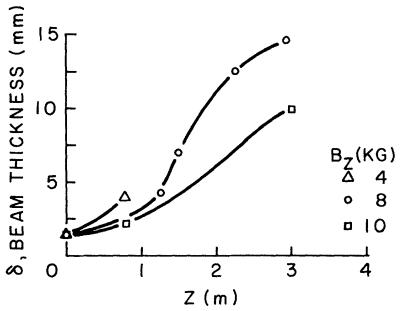

FIG. 2. Thickness of the annular electron beam as a function of axial distance along the drift tube.

ial distance for various field strengths. For the range of fields used the breakup of the beam is reduced as the field strength is increased. Instability growth rates for the spread in beam size are about 10^9 sec^{-1}. The plotted points indicate the maximum beam dimension and may overestimate the beam size, especially at early times when the beam is most concentrated.

The breakup of the beam is accompanied by an intense burst of microwave radiation (monitored in the X band). The signal strength exceeds that found in short tubes (0.75 m) by a factor of about 500 at 4 kG and decreases monotonically as the field increases, to a factor of less than 10 at 10 kG. The fall in intensity at high field strengths arises partially from the radiated frequency increasing until it is out of the bandwidth of the receiver used. The spectrum of the radiation is shown in Fig. 3 for various field strengths and its frequency content is compared to the radiation from similar beams in the short (0.75 m) tube. In this case the radiation is driven by an anisotropy instability[9,10] and occurs as a backward wave when the phase velocities of the TE_{01} waveguide mode and beam cyclotron modes are equal. This occurs at a frequency

$$\omega = \frac{\Omega_c}{1-\beta^2}\left\{1-\beta\left[1-(1-\beta^2)\frac{\omega_{co}^2}{\Omega_c^2}\right]^{1/2}\right\}, \qquad (1)$$

where $\Omega_c = eB/\gamma m$ and ω_{co} is the guide cutoff frequency.

Faraday cups were used to measure the drifting beam current at the end of the short (0.75 m) and long (3.0 m) drift tubes. The results of these measurements are shown in Fig. 4. The duration of the beam current at the end of the long tube is only half of that observed at the end of the 0.75-m tube. Consequently the beam loses approximately three quarters of its initial energy in transit through the last 2 m of the tube. It should

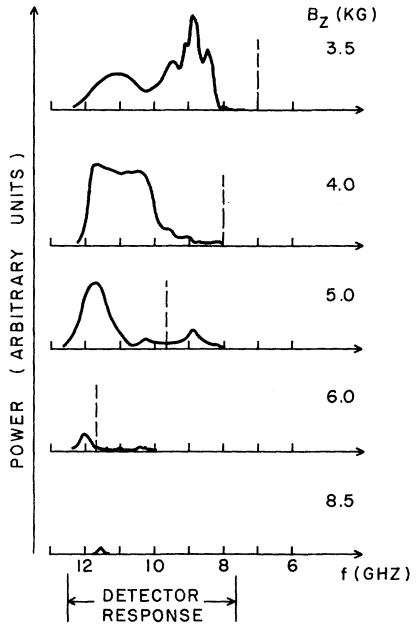

FIG. 3. X-band radiation spectrum from an unneutralized beam in a 3-m-long drift tube. The dashed line represents the frequency of the radiation monitored in a short (0.75 m) drift tube.

be pointed out that at the base pressures used, the beam is unneutralized and the current flow is limited[5,6] by the space-charge depression of the potential within the tube. Calculations yield limiting currents very close to the 7–8 kA observed. The remaining diode current does not contribute to the beam but is expelled to the drift-tube well. The low beam current monitored is limited by the beam location with respect to the tube wall.

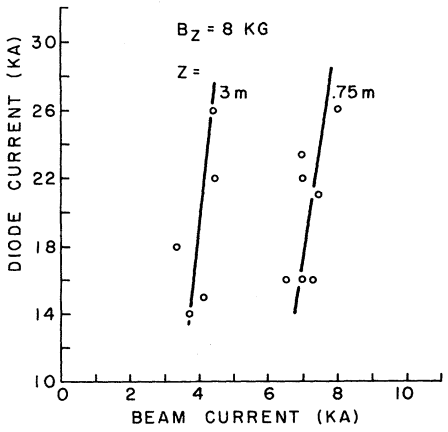

FIG. 4. Faraday-cup measurements of the beam current at two positions (0.75 m and 3.0 m) along the drift tube. Beam injection energy, 400 keV.

A similar beam located at the tube wall would carry a beam current of about 40 kA. It is possible that some space-charge neutralization exists, which would serve to increase the beam current. The observed characteristics make it very probable, however, that complete space-charge neutralization has not been achieved and that the beams used exhibit the shear characteristics associated with space-charge–depressed propagation. Experiments and calculations reported elsewhere[6] support these statements.

We now briefly discuss the mechanisms which could lead to the observed beam breakup. The beam current, which is increasing throughout the voltage pulse, has to provide both the particle and field energy. These fields, both electrostatic and electromagnetic, lead to the slowing down of the beam particles through an induced axial field. This field, which also increases the shear in the beam axial velocity, interacts with the self-field of the beam in a sense tending to expel the particles from the beam. This is the opposite sense to that observed experimentally. The time taken to establish these fields is about 30 nsec.

Anisotropy in the beam temperature can be ruled out as the instability mechanism, as experimentally increasing the ratio $T_\perp/T_\parallel$ by injecting the beam through thin foils does not lead to more rapid breakup of the beam.

Explanations based on the cyclotron-wave instability and a slowing down of the beam electrons are inconsistent with the radiation emitted. Any loss of electron energy would result [see Eq. (1)] in the emission of higher-frequency radiation from the beam, not lower as observed in the long tube. The remaining mechanisms are mainly of the Diocotron family and have been described in the literature by Kyhl and Webster,[11] Rome and Briggs,[12] Levy,[13] and others. Kyhl and Webster have also performed experiments in milliampere, 80-V beams which show similar trends to those reported here. In the existing calculations the instability is treated from the point of view of orbit theory (i.e., assuming $\omega_p^2/\omega_c^2 \ll 1$). In our experiments this parameter has a value of about unity. Other effects present in our experiments which should be considered in a detailed calculation include the proximity of the walls, relativistic effects, beam shear, and self–magnetic-field effects. In spite of these limitations the basic trends predicted by the theories, i.e., the instability growth length and the stabilizing effects of stronger guide fields, are quantitatively consistent with experiment. The real part of the frequency for this instability occurs at a frequency of the order of the azimuthal mode number times the rotational velocity of the beam. The observations made show that the instability produces radiation at frequencies in this range. A difficulty in the above interpretation arises from the static patterns observed on the witness plates. The instability discussed by Rome and Briggs entails a traveling helical wave. The static patterns observed could be accounted for by an irregularity in the drift tube determining the spatial location of the unstable beam. A possibility which avoids this problem has been proposed by Sudan[14] who observes that an azimuthal perturbation in the beam current will induce a corresponding perturbation in the return-wall current. This can drive the particles inward provided that a fractional charge neutralization greater than γ^{-2} is achieved. Our beam observations are consistent with the retention of space charge, but cannot preclude the possibility of a fractional charge neutralization as required by this model.

Finally, we consider the question of the beam instability developing on the inside surface of the system. In the Sudan model this occurs naturally provided the space-charge–neutralization condition is satisfied. In the sheared-flow instabilities we note that the unstable surface can be controlled by the proximity of conducting walls. In the experiment, the drift-tube wall is close to the beam location and will tend to minimize azimuthal and axial electric fields on the outer surface of the beam and, consequently, result in preferential growth on the inner surface of the beam.

These observations of beam breakup are relevant to plasma injection, to electrostatic confinement and heating schemes, and finally to high-power microwave generation devices, and impose limits not clearly defined in the past.

We are grateful to Professor Ott and Professor Sudan for helpful discussions on instability mechanisms. The experimental help afforded by Dr. A. Fisher and Mr. M. Read is also gratefully acknowledged.

This work was supported by the National Science Foundation.

[1]R. V. Lovelace and R. N. Sudan, Phys. Rev. Lett. 27, 1256 (1971).

[2]M. V. Babykin, E. K. Zavoiskii, A. A. Ivanov, and L. I. Rudakov, in *Proceedings of the Fourth Internation-*

al Conference on Plasma Physics and Controlled Nuclear Fusion Research, Madison, Wisconsin, 1971 (International Atomic Energy Agency, Vienna, 1972), paper No. CN-28/D10.

[3]C. B. Wharton, private communication.

[4]M. L. Andrews, H. Davitian, H. H. Fleischmann, B. R. Kusse, and J. A. Nation, Phys. Rev. Lett. 27, 1428 (1971); J. J. Bzura, T. J. Fessenden, H. H. Fleischmann, D. A. Phelps, A. C. Smith, Jr., and D. M. Woodall, Phys. Rev. Lett. 27, 256 (1971).

[5]L. S. Bogdankevich and A. A. Rukhadze, Usp. Fiz. Nauk 103, 609 (1971) [Sov. Phys. Usp. 14, 163 (1971)].

[6]J. A. Nation and M. Read, Bull. Amer. Phys. Soc. 18, 585 (1973), and to be published.

[7]M. Friedman and M. Ury, Rev. Sci. Instrum. 41, 1334 (1970).

[8]M. Friedman and M. Herndon, Phys. Rev. Lett. 28, 210 (1972), and 29, 55 (1972).

[9]Y. Carmel and J. A. Nation, Bull. Amer. Phys. Soc. 18, 586 (1973), and to be published.

[10]E. Ott and W. Manheimer, Bull. Amer. Phys. Soc. 18, 4, 585 (1973).

[11]R. L. Kyhl and H. F. Webster, IRE Trans. Electron Devices 3, 172 (1956).

[12]J. A. Rome and R. J. Briggs, Phys. Fluids 15, 796 (1972).

[13]R. H. Levy, Phys. Fluids 8, 1288 (1965).

[14]R. N. Sudan, private communication.

Effect of the Trapped-Particle Instability on Toroidal Plasma Confinement*

J. A. Schmidt

Plasma Physics Laboratory, Princeton University, Princeton, New Jersey 08540

(Received 6 April 1973)

A stability condition is derived for the trapped-electron instability which is valid in both the collisional and collisionless regimes. This instability arises from wave-particle interaction between the perpendicular phase velocity of the waves and the gradient-B drift velocity of the electrons. The stability condition is applied to the FM-1 spherator and ST and PLT tokamaks.

Particle-loss rates have been observed in the FM-1 spherator which exceed those which are predicted by classical collisional diffusion.[1,2] This discrepancy between classical and observed diffusion increases when particles are trapped in regions of medium or low shear ($L_s/a \simeq 30$) and unfavorable curvature. Since this anomalous loss occurs under favorable minimum-B as well as high shear conditions, its source will likely prove important in any toroidal system. Correlations between the fluctuating density and electric field have been determined; these indicate a turbulent diffusion coefficient which is sufficient to explain the observed loss.[3]

The confinement time is reduced when the particles are mirror trapped at large major radius outside the internal ring, where the shear is low and the magnetic field curvature unfavorable.[4] A set of plasma and machine parameters at which anomalous loss occurs are given in Table I. These parameters are appropriate to the region at larger major radius than the internal ring where the fluctuations are observed.

The following assumptions will be made in developing a theory which is compatible with the experimental conditions. The energy driving the instability will come from trapped electrons. The ions and untrapped electrons will produce a dielectric medium giving drift-wave propagation with real frequencies governed by the well-known dispersion relation[5]

$$\omega^2 - I_0 e^{-b}(\omega\omega^* + k_\parallel^2 C_s^2) \times [1 - T_e/T_i(I_0 e^{-b} - 1)]^{-1} = 0, \quad (1)$$

where $b = (k_x^2 + k_y^2)\rho_i^2/2$, $\rho_i \equiv (m_i v_i/eB)$, $\omega^* \equiv k_y \kappa T_e/eaB$, $C_s = v_i(T_e/T_i)^{1/2}$, and a is the density scale length. We assume that the turbulence originates in the region of particle trapping with a wave number $k_\parallel$ parallel to $\bar{B}$, k_y perpendicular to $\bar{B}$ and the density gradient, and a wave packet in the direction of the density gradient characterized by a wave number k_x. The effect of magnetic field

TABLE I. FM-1 parameters.

Peak density	10^{11} cm^{-3}
Electron temperature	2 eV
Ion temperature	1 eV
Density scale length a	3 cm
Field curvature R	~21 cm
Field strength	$\sim 2k\Gamma$
Shear length L_s	~80 cm
Electron bounce frequency	5×10^6 Hz

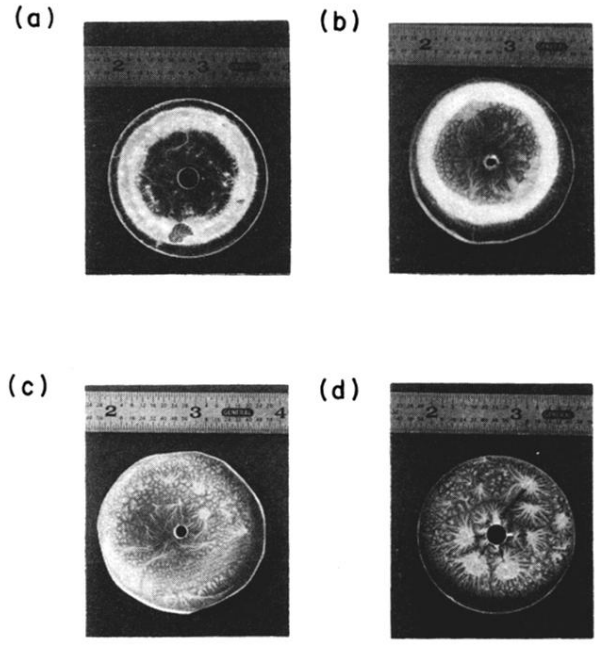

FIG. 1. Witness plates mounted at (a) 0.75 m, (b) 1.2 m, (c) 1.5 m, and (d) 3.0 m along the drift tube. The beam remained centered in the tube in all cases.